Plasmonics
https://doi.org/10.1007/s11468-024-02410-5

RESEARCH

Amla (*Emblica officinalis*)-Derived Bionanosilver (Ag NPs) for Excellent Antibacterial Activity

Amar Nath Yadav[1] · Pallavi Singh[2] · Shiva Upadhyay[3] · U. P. Tyagi[4] · Ashwani Kumar Singh[4] · Pushpa Singh[2] · Amit Srivastava[5]

Received: 10 May 2024 / Accepted: 25 June 2024

Abstract

Despite the growing need for effective and environmentally friendly antimicrobial agents, the synthesis methods for such materials often involve toxic chemicals and complex procedures. There is a pressing need for a sustainable approach to synthesize nanoparticles with potent antibacterial properties. This study aims to address this gap by developing a green synthesis method for silver nanoparticles (Ag NPs) using Amla extract. Powder X-ray diffraction (XRD), UV–Vis absorption spectroscopy, and Transmission Electron Microscopy (TEM) demonstrated that face-centered cubic Ag NPs with sizes in the range of 15–30 nm can be synthesized through an environmentally friendly process. Further, the formation mechanism of Ag NPs has been discussed in detail with the help of schematic diagrams. The Amla-derived Ag NPs have been further tested for their antibacterial activity against two different antibacterial strains: *Escherichia coli* (*E. coli*) and *Staphylococcus aureus* (*S. aureus*) using the plate count method. The NPs showed excellent biocompatibility where approximately 90% of growth reduction have been found for both strains at 100 µg/mL of Ag NPs and growth time of 30 min. These outcomes exhibited that Ag NPs, as a kind of antibacterial material, had an incredible guarantee for application in a wide scope of biomedical applications.

Keywords *Phyllanthus emblica* (Amla) · Silver nanoparticles · Antibacterial activity *Escherichia coli* (*E. coli*) · *Staphylococcus aureus* (*S. aureus*)

Introduction

Microorganisms can quickly develop in our environment as they contaminate oceans, soil, and air. In a short while, a multistep process starts and forms a complex microbial community known as a biofilm. Biofilms can have more than 99% of bacteria attached to their surfaces. Moreover, bacterial biofilms are sheltered from antibiotics and phagocytosis, making them difficult to control clinically. This results in several diseases, including hygienic problems and chronic infections, due to biofilm formation. Thus, antibacterial materials and agents play an essential role in controlling microorganisms. Thereby, we need an effective and non-toxic antibacterial agent that can resist microorganisms [1, 2].

In recent years, the synthesis of metallic nanoparticles (NPs) with tunable shapes and sizes has attracted much attention because of their significant applications in various fields of science [3, 4]. Due to their very high surface-to-volume ratio, these metallic NPs exhibit unique optical, electrochemical, catalytic, and biological properties [5, 6]. In particular, these metal NPs have been used in applications such as surface-enhanced Raman spectroscopy (SERS), gene delivery systems, and artificial implants [7–12]. Among metal NPs, silver nanoparticles (Ag NPs) are one of the most crucial and captivating nanomaterials in biomedical

✉ Ashwani Kumar Singh
asingh22@db.du.ac.in

✉ Pushpa Singh
pushpasingh@ramjas.du.ac.in

[1] School of Physical Sciences, Jawaharlal Nehru University, New Delhi 110067, India

[2] Department of Botany, Ramjas College, University of Delhi, Delhi 110007, India

[3] Department of Physics, Swami Shraddhanand College, University of Delhi, Delhi 110036, India

[4] Department of Physics, Deshbandhu College, University of Delhi, New Delhi 110019, India

[5] Department of Physics, TDPG College VBS Purvanchal University, Jaunpur 222001, India

Published online: 08 July 2024

applications. Ag NPs play a significant role in nanoscience and nanotechnology, especially in nanomedicine. Although several noble metals have been utilized for various purposes, Ag NPs have been focused on likely applications in cancer diagnosis and therapy. Moreover, Ag NPs have recently been used as a potent antibacterial agent in many bactericidal applications [13].

A variety of synthesis techniques have been developed to blend metal NPs, including chemical reduction, solvothermal, sol–gel processes, and laser dissipation. However, these techniques have certain constraints, including the use of hazardous reductants or complex and costly instruments. Therefore, environmentally friendly nanoparticle synthesis protocols have come into focus. Among the different microorganisms, prokaryotic microorganisms were first acknowledged to have potential in the biosynthesis of NPs. Beveridge and Murry were among the first to demonstrate the formation of octahedral gold particles with nanometric dimensions [14]. The silver-resistant bacterial strain *Pseudomonas stutzeri* AG259 accumulates silver nanoparticles along with some silver sulfide in the cell, with particle sizes ranging from 35 to 46 nm [15]. Several eukaryotes like fungi and yeast have also been explored for the synthesis of metal and metal oxide NPs [16–18]. Plant extracts have also demonstrated significant potential for the rapid synthesis of metal NPs and are being used widely due to the better-understood mechanisms of NP synthesis with plant extracts compared to fungi, yeast, or microorganisms [19]. Various plant extracts, such as *Chenopodium album* leaf [20], *Cinnamomum camphora* [21], *Ficus benghalensis* [22], *Hypericum perforatum* [23], and many others [24–41], have generally been utilized for the synthesis of different metallic NPs. The use of plant extracts is preferable to synthetic compounds because of their low cost, availability, and ecocompatibility. Additionally, plant extracts allow for a faster and simpler procedure for Ag^{+} reduction compared to conventional chemical methods.

Phyllanthus emblica, commonly known as "Amla," is a popular fruit tree originating in India and is considered beneficial for health due to the presence of various nutraceuticals (calcium, vitamin C, lysine, minerals, phosphorus, etc.) and its ability to fight many human diseases [59]. Currently, it is cultivated in small agro-forest industries in many tropical and subtropical countries because of its use in many pharmaceutical products. However, the nutritional, pharmaceutical, and chemical features of Amla open the way to novel, interesting processes involving *Emblica officinalis*, allowing for its full potential to be exploited. To the best of our knowledge, Ag NPs derived from Amla extract have not been deeply investigated so far [42–44]. The low number of papers on this topic highlights the novelty of this work. The growing interest in Ag NPs as antibacterial agents is evidenced and justified by their immediate biomedical application and the green synthesis methodology. Notably, the general topic "silver nanoparticles" and "Streptococcus pyogenes" has grown from 2009 to 15 papers in 2020. However, the number of papers is still low, and novel results are required to enable practical applications of Amla-derived Ag NPs as antibacterial material.

This study addresses many current limitations in tackling bacterial infections, such as antibiotic resistance, toxicity, and biofilm formation. In this work, we used *Emblica officinalis* extract to prepare Ag NPs for use as an antibacterial agent against two different bacterial strains, namely, *E. coli* (Gram-negative) and *S. aureus* (Gram-positive). The results demonstrate that an easy, green, and environmentally friendly fabrication process using Emblica extract produces an efficient antibacterial agent, even with low Emblica concentrations during the reduction process. A clarification on the reduction mechanism of silver ions and NPs formation is also provided, highlighting the broad-spectrum activity, high efficacy, and biocompatibility of Amla-derived Ag NPs. These findings suggest that Amla-derived Ag NPs have significant potential for various biomedical applications, including wound healing, medical device coatings, and drug delivery systems, offering a sustainable and effective solution for preventing and treating bacterial infections.

Materials

Silver nitrate ($AgNO_3, \geq 99.0\%$ purity) was procured from sigma Aldrich. Luria- Bertani (LB) medium and Agar powder, used for culture was supplied from HiMedia Laboratories, India. Dried amla powder was purchased from local market. DI water is used for the synthesis of Ag NPs (18MΩ).

Methods

Synthesis

Silver nanoparticles (Ag NPs) were synthesized via a reaction of $AgNO_3$ with *Phyllanthus emblica* (Amla) extract. Amla extract was prepared by simply dipping 5 mg of dried Amla powder for 24 h into 100 mL of double-distilled water. The solid content was filtered out, leaving the residual extract of dark brownish color. This extract was further used in consecutive steps for the synthesis of Ag NPs. In a typical synthesis method, first, an aqueous solution (50 mL) of $AgNO_3$ with molarity 0.1 M was prepared. After that, 50 mL of Amla extract was added to solution under vigorous stirring. Further, after a few minutes, the reaction changed to faint brownish color, which indicates the formation of Ag NPs. Finally, the Ag NPs were collected by centrifugation,

washed several times, and redispersed in water. Similarly, by varying the concentration of Amla extract (25 mL, etc.) in the aqueous solution of $AgNO_3$ (same concentration 50 mL and 0.1 M), other samples were prepared.

Characterizations

XRD analysis of resulting samples was carried out with an X Pert Pro X-ray diffractometer (PAN analyst BV the Netherlands with a build in graphite monochromatometer) with Cu Kα radiation ($\lambda = 1.54056$ A°). The samples for XRD were prepared by placing one drop of reaction mixture on a circular disk (5-mm diameter) and allowing it to dry. Transmission election microscopic (TEM) images were captured on JEOL microscope at an accelerating voltage 200 keV. The UV–Visible spectroscopic measurements were carried out with the Perkin Elmer Lambda 750S UV–Visible spectrometer.

Antibacterial Study

Study of antibacterial activity of Ag NPs was performed on two bacterial strains, viz. *E. coli* and *S. aureus* (all clinical strains). The component of Luria–Bertani (LB) medium was used in growing and maintaining the bacterial culture. The effect of Ag NPs on bacteria was investigated by culturing the organism on LB plates (10^5 colony-forming units per plate), along with Ag NPs with different concentrations, i.e., 20, 40, 60, 80, and 100 µg/mL of the media. Plates without Ag NPs were taken as control. Plates were incubated for 24 h at 37 °C, and the colonies were controlled for achieving results. The counts of three plates corresponding to a particular sample were averaged to obtain the result. The growth of bacteria in the liquid broth was studied in LB media; inoculation was given from fresh colonies on agar plates into 50 mL of media. The media containing 10^5 cells/mL was adjusted for the 0th minute of reading (Spectrophotometer Bio-Rad Smart plus). Readings were taken at an interval of 15 min at 600 nm.

Results and Discussion

Structural and Morphological Characterization of Ag NPs

Figure 1 shows a simplified pictorial illustration of the process employed to synthesize Ag NPs. After adding Amla extract to a 0.1 M aqueous solution of $AgNO_3$, the mixture changed to a brownish color within 4–5 min of reaction. The change in color of the reaction mixture indicates the formation of Ag NPs.

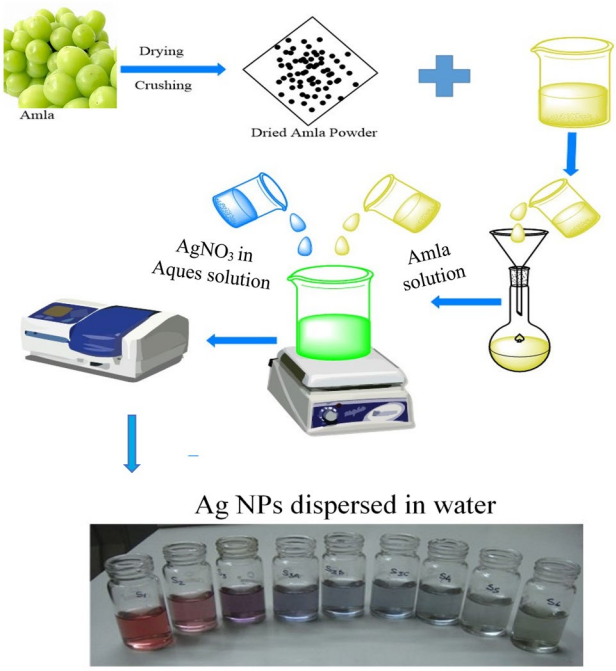

Fig. 1 Schematic illustration of the procedure used to synthesize of colloidal Ag NPs from $AgNO_3$ solution

Figure 2 shows the powder X-ray diffraction pattern (XRD) pattern of the Ag NPs prepared at a concentration of 1:1 ($AgNO_3$: Amla extract). The diffraction pattern, recorded in the 2θ range 10–80°, shows four strong Bragg's diffraction around 2θ values of 38.45°, 46.35°, 64.75°, and 78.05° corresponding to the (1 1 1), (2 0 0), (2 2 0), and (3 1 1) planes, respectively. According to this analysis, we can conclude that the sample has an FCC structure. Moreover, corresponding to the observed diffraction planes the interplanar spacing also calculated and found to be 2.33,1.95, 1.43 and 1.22 Å for (1 1 1), (2 0 0), (2 2 0), and (3 1 1) planes, respectively. A strong increase in crystallinity can be observed for the 1:1 ($AgNO_3$: Amla extract) value. The reason for this observation can be found in the larger crystallite size of 1:1 ($AgNO_3$: Amla extract) samples that provide enhanced number of parallel planes for the XRD diffraction. The average crystalline size has been estimated by the Debye–Scherrer formula:

$$L = (0.9 \times \lambda)/(\beta \times \cos\theta)$$

where λ (= 1.54 Å) is the wavelength of X-rays, β is the full width of half maxima (FWHM) in radians, and θ is Bragg's angle. The FWHM for the plane (111) at 2θ value of 38.45° is found to be 0.293 and 0.518 for 1Ag:0.5A and 1Ag:1A ratios, respectively. Thus, average crystalline sizes of about 17 nm and 30 nm have been calculated, respectively. These results agree with literature reports on the synthesis of Ag

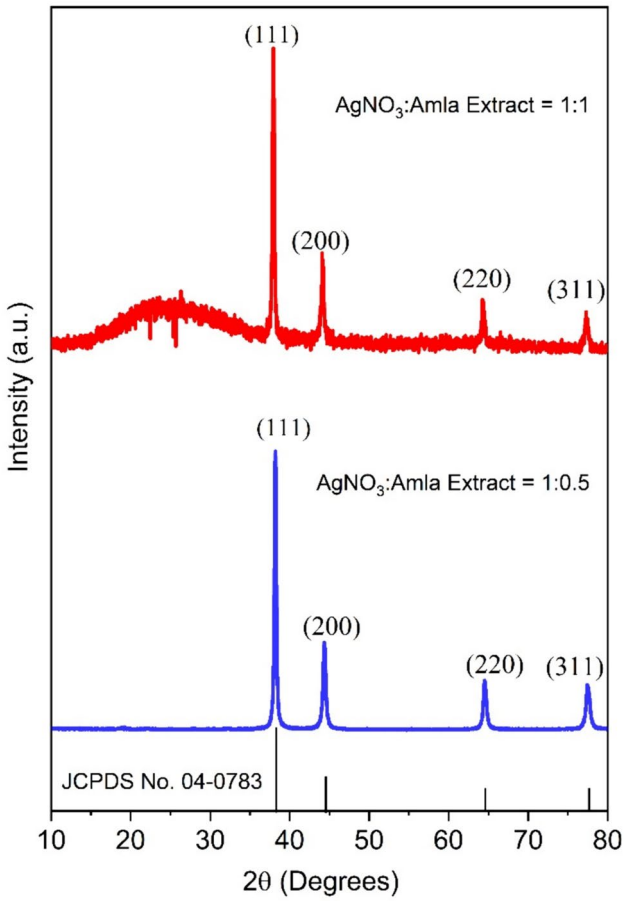

Fig. 2 XRD pattern of Ag NPs at different concentrations of $AgNO_3$ and Amla extract

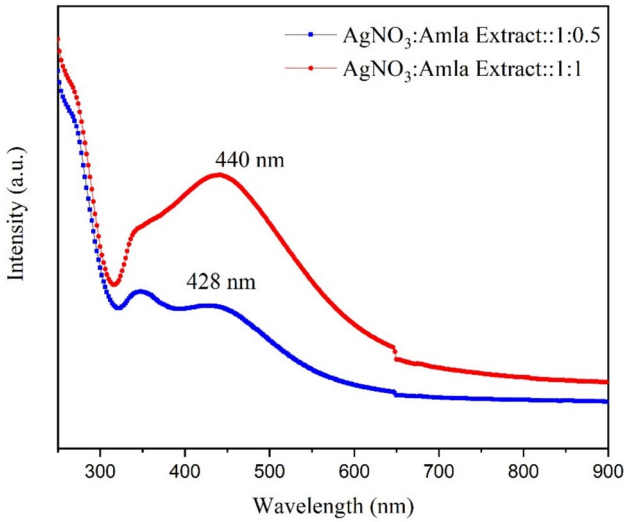

Fig. 3 UV–Vis absorption spectra of Silver (Ag) NPs with different concentrations of Amla extract

NPs using various plant extracts [19, 45, 46], where it is explicitly demonstrated the dependence of particles size on the mixing ratio of $AgNO_3$ solution and plant extract. As the amount of extract is reduced, the particle size gets smaller and smaller.

Figure 3 depicts UV–Visible absorption spectra of Ag NPs measured at two concentrations, i.e., $AgNO_3$: Amla extract = 1:0.5 and 1:1, respectively. The curves show a broad absorbance around 428 nm for sample 1Ag:0.5A and at 440 nm for 1Ag:1A sample attributed to surface Plasmon resonance (SPR) [47–49]. Ag NPs have very close conduction and valence band in which electrons are supposed to move freely. When the sample is illuminated with electromagnetic light of specific wavelength, these free electrons give rise to a SPR absorption band, arising due to the collective oscillation of conduction electrons of Ag NPs in resonance with the light wave. The absorption band of Ag NPs is depends on various parameters such as nanoparticle size, chemical surrounding and dielectric medium. Depending on this absorption band, the size of the NPs ranging from 10 to 100 nm can be estimated. Furthermore, using the UV–vis spectroscopy, the stability of Ag NPs as prepared from biological method has been checked and found similar characteristic after the 12 months. Thus, we can conclude that as prepared Ag NPs using Amla extract is highly stable.

The redshift observed at the high concentration of Amla extract clearly indicates the correspondent increase in the size of Ag NPs, in agreement with literature [48] and our XRD results. Also, the peak centered at 440 nm has higher FWHM for 1Ag:1A sample, suggesting the formation of poly dispersed NPs in 1Ag:1A and mainly of spherical shaped particles in 1Ag:0.5A condition. As demonstrated by Mie's theory [49], the presence of only one SPR band can be indicative of a spherical shape, while the detection of other bands suggests the formation of other shapes (for example triangular nanoplates, disks) of metal NPs. Accordingly, the second absorption band at around 350 nm with no significant shift with Amla concentration can be attributed to the presence of other morphologies of Ag NPs [50], as confirmed by direct measurements of Ag NPs size by TEM analysis.

In Fig. 4a–d, TEM images of Ag NPs at two different magnifications and two different concentrations of Amla extract are reported. The analysis of the TEM micrographs evidences that NPs are spherical and well dispersed over the grid. At high concentration of reducing agent (1:1/$AgNO_3$: Amla extract), the average size of spherical NPs has been estimated in the range of 25–30 nm, and many polydispersed NPs in the form of nanotriangles or prisms are noted (Fig. 4a, b). As shown in Fig. 4c, d, by reducing the concentration of Amla (1:0.5), the size of the spherical Ag NPs becomes smaller down to about 15–20 nm, and less nanotriangles are detected. The analysis of histogram plots (Fig. 4e, f) shows that average particle size increases with

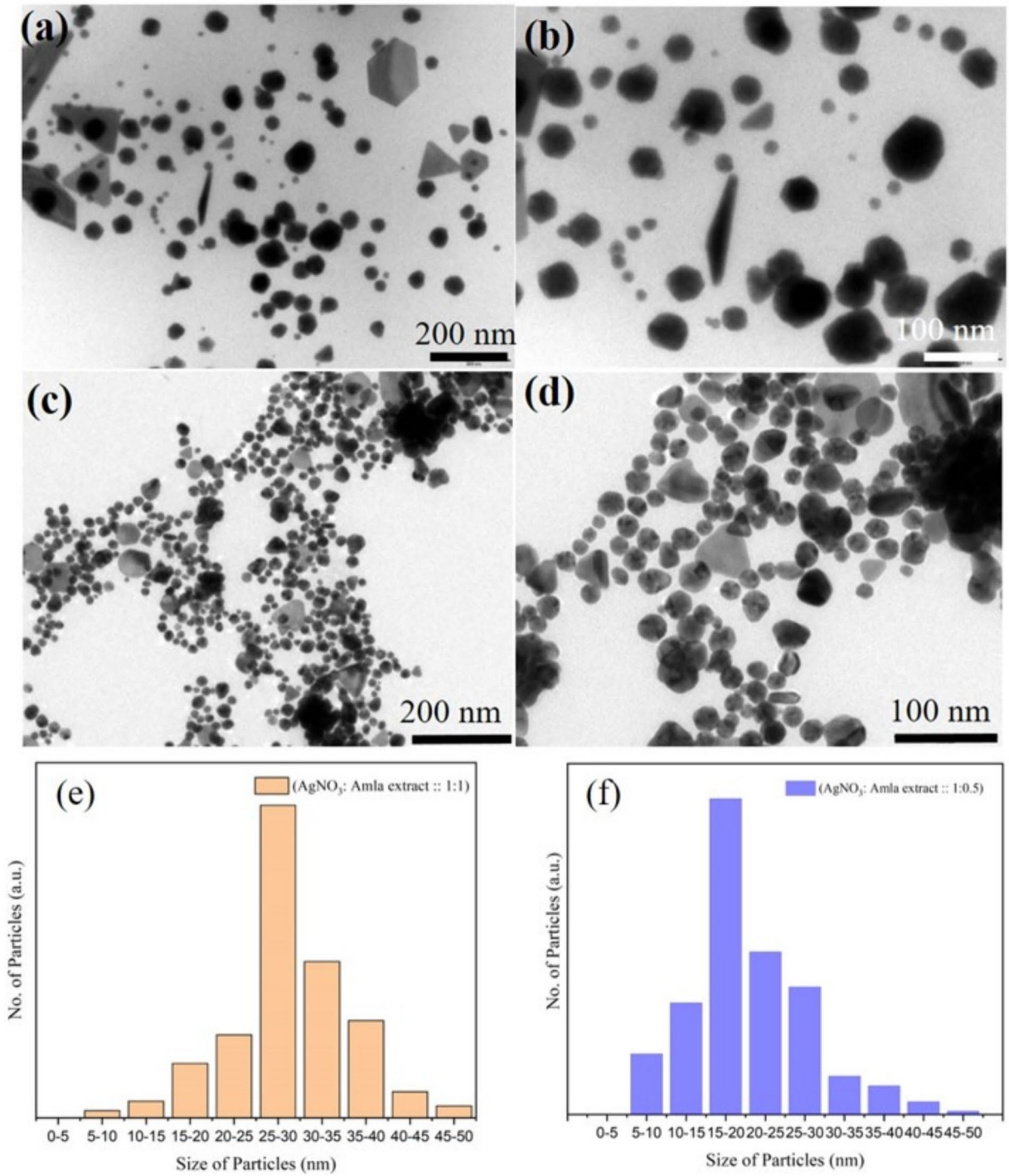

Fig. 4 TEM images of Ag NPs at different concentrations of $AgNO_3$: Amla extract: **a, b** 1:1 and **c, d** 1:0.5. (**e, f**) Corresponding histogram plots of nanoparticle size distribution

the decrease of the ratio of Amla extract with respect to $AgNO_3$. These results clearly shown that here Amla act as a reducing as well as a stabilizing agent in the synthesis of Ag NPs. Further, the sizes obtained from TEM analysis were well matched with absorbance spectra (Fig. 3) and XRD results (Fig. 2) and with literature data of both samples [51].

Mechanism of Ag NPs Formation

The mechanism of nanoparticle formation consists of three main steps: (i) reduction of ions, (ii) nanoparticle nucleation and growth, and (iii) nanoparticle stabilization.

Notwithstanding the mechanism of bioreduction and capping of metal ions by plant extracts is not completely clarified in literature [52–56], the reduction ability of Amla extract can be certainly ascribed to the high content of phenolic compounds, namely, gallic acid, methyl gallate, 3–6-di-O-galloyl-glucose, mucic acid gallates, flavonoids (as quercetin), and acid ascorbic that have been identified in many papers [57–59]. In addition, another antioxidant phenolic compound, Hamamelitannin, has been extracted for the first time from Phyllanthus emblica very recently [60]. The functional groups of these phytomolecules are recognized not only to be responsible of metal ion reduction but also to stabilize and make biocompatible the resulting Ag NPs. The capability of natural polyphenol compounds to reduce silver ions has been recently confirmed by Ferraris et al. in a work on bioactive glasses [61]. It is known that the mechanistic aspects of the chemical reduction reaction by plant/fruit extracts are difficult to understand due to the complexity of the biological systems, and thus, it remains a big challenge that requires more detailed studies [62, 63]. On the base of these considerations, a probable mechanism of Amla-derived Ag NPs formation is here discussed with the attempt to unify and discuss the fragmental information reported in literature on the base of experimental results.

According to some authors [64, 65], the process of silver ion reduction (first step) is strictly correlated to the keto-enol tautomerism [66] of the polyphenol constituents. All these compounds possess many hydroxyl groups in their aromatic rings, as illustrated in Fig. 5, where the chemical structure of the main constituents identified in Amla extract [57] is reported. As shown in Fig. 5, silver cation is presumably attracted by oxygen of the O–H groups forming intermediate single charged complex that then transforms into the keto-form of the polyphenol compound releasing Ag ions, hydrogen ions, and electrons [67]. Then, the reduction of Ag^+ by direct acceptation of electrons (Eq. 1 in Fig. 6a) or via molecular hydrogen produced by H^+ reduction (Eq. 2 in Fig. 6b) takes place [67].

Since our results confirm that NPs are formed in short times (4–5 min), the mechanism of nanoparticle formation can be plausibly ascribed to autocatalytic reduction—nucleation, nucleation—growth, Ostwald ripening, and coalescence in agreement with literature [68]. We have schematized this process in Fig. 6b. The initially formed silver metal atoms undergo to autocatalytic reduction. Silver atom and silver ion form Ag_2^+ clusters that react each other forming Ag_4^{2+} ions, and finally Ag_4^{2+} clusters interact with polyphenol compounds giving Ag/polyphenol complexes [69]. Then, these complexes interact each other forming a small metal

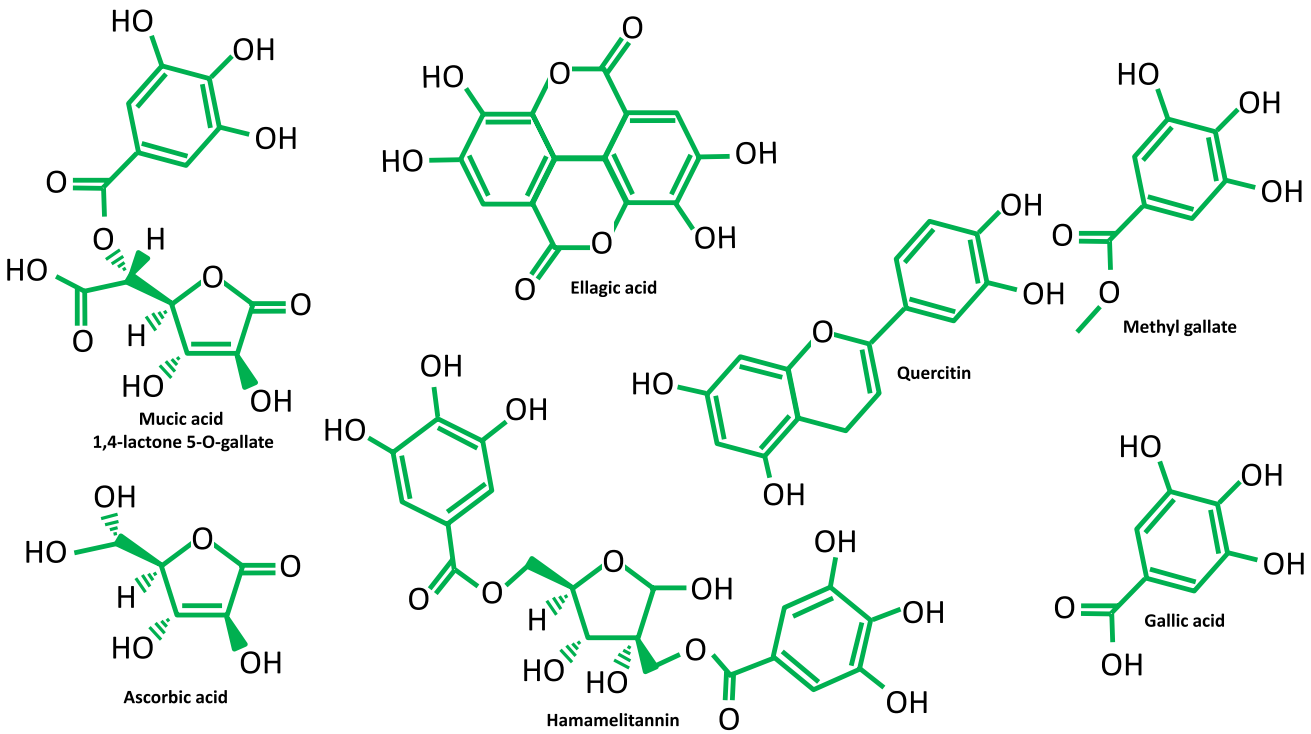

Fig. 5 Chemical structure of the most important reducing constituents extracted in fruits of *Emblica officinalis* (Amla) [57]

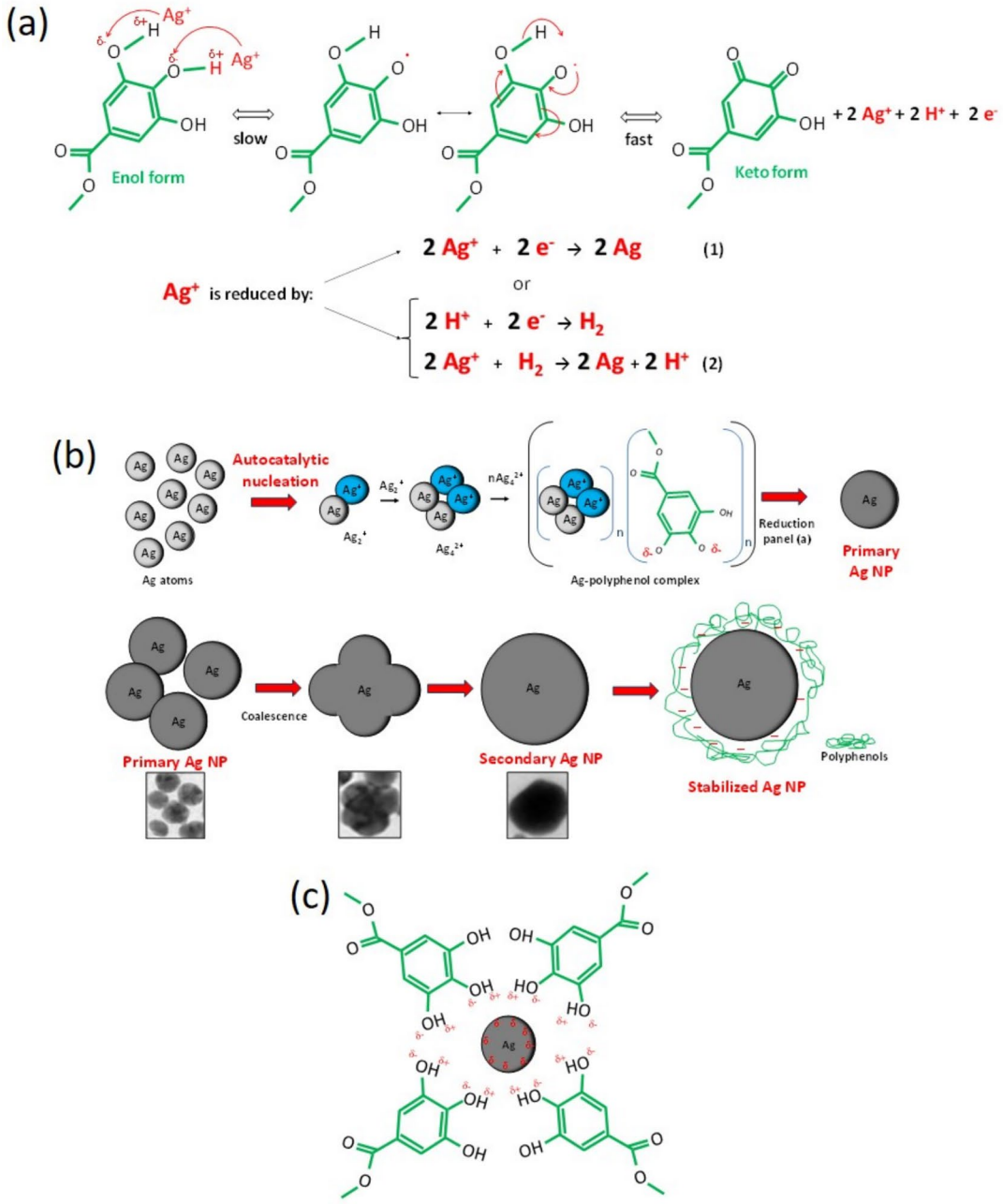

Fig. 6 Schematic illustration of **a** the hypothesized mechanism of chemical reduction of Ag^+ ions to Ag metal atoms, **b** process of NPs nucleation and growth, and **c** chelation of Ag NPs by polyphenols that prevent agglomeration

(primary) nanoparticle by chemical reduction. This mechanism is supported by experimental data suggesting that polyphenols are involved not only in bioreduction but also in the nucleation of nanoparticle formation and subsequent aggregation thanks to their ability to adsorb on the silver surface [64]. After that, a process of primary NPs thickening occurs by coalescence and Ostwald ripening. Particles increase their size more, and more until the stabilization process takes place.

The stability of the formed Ag nanoparticle is attributed to presence of -OH and = O groups or π-electrons in polyphenols that behave as electrostatic inhibitors of particles coalescence and aggregation by forming a coating around the particle [70–74]. For example, it is reported that quercetin, contained in Amla extract, possess great chelating ability, thanks to the simultaneous action of carbonyl, hydroxyl, and the catechol groups that bond with metal particle [64]. Other experimental data confirm that phenolic compounds,

such as mucic acid-1,4-lactone-3-O-gallate, ellagic acid, and isocorilagin in methanolic extracts from Amla could chelate ferrous ion [73]. Since Ag NPs have a negative zeta potential value in their pure form [67], a possible mechanism of silver particle capping should involve for the main part the interactions between hydrogen atom of the -OH groups and silver metal [75], as schematized in Fig. 6c.

In order to have a good dispersion of Ag NPs, additives are often added to the synthesis solution to hinder particle growth and agglomeration by electrostatic and steric stabilization effects [76]. According to the stabilization allowed by polyphenols, that show the double functionality of reduction and stabilizing agent, the addition of stabilizing additives in the initial solution of synthesis is not necessary. In our results, the formation of stabilized nanoparticle is confirmed by TEM analysis that show a quite narrow distribution of particle sizes at both the investigated ratios (Fig. 4).

Antibacterial Activity

Figure 7 is the optical image of petri plates used to study the growth of two different bacterial strains, namely, *E. coli* and *S. aureus*, respectively, at three different concentrations showing different stages of bacterial growth. Figure 7a is a set of three photographs showing the effect of silver nanoparticles on *E. coli* at different concentrations. The first plate shows the growth of bacterial in the medium when there was no Ag NPs used (control). In this plate, we can see an enormous number of bacterial colonies, grown over the medium uniformly. The second and third images of this set are the images of plates when 40 and 80 µg/mL concentrations of Ag NPs were used. Here we can see that the growth of bacterial colonies has been restrained significantly for 40 µg/mL concentration of Ag NPs, whereas for 80 µg/mL concentration, there is almost no growth in colony of bacteria. Similar results were found for *S. aureus* which is shown in Fig. 7b. The first plate is again a control plate which shows high growth of Bacteria. Bacterial colony growth gets severely affected as we keep on increasing the concentration of Ag NPs as evident from the images. Since at 80 µg/mL concentration of Ag NPs effectively siege the growth on bacteria, photographs containing higher concentration of Ag NPs have not been shown in Fig. 7. A separate experiment to study the effect of pure amla extract on the growth of bacterial strains (*E. coli*) was done. It was found that pure amla extract offer almost no bacterial growth inhibition (shown in plate photograph 7c).

The dynamics of bacterial growth was observed in liquid LB media. For control, we have used LB-media containing no Ag NPs. We further mixed different concentrations of Ag NPs such as 20, 40, 60, 80, and 100 µg/mL in LB-media and then checked bacterial growth in the two different strains. It is well known [77, 78] that smaller size particles offer more surface area and thus enhanced number of active sites as compared to their larger counterpart, thus NPs, synthesized with ratio $AgNO_3$: Amla extract 1:0.5, were used for the antibacterial activity studies.

At a 15-min interval, we took readings for bacterial growth. At all concentrations of Ag NPs, we found a decrease in the growth of each bacterium over the time. As shown in Fig. 8, at greater nanoparticle concentrations, the rate of growth suppression is substantially faster. In comparison to Gram-negative bacteria, the growth suppression of Gram-positive bacteria was rather minor. The log phase of the gram-negative bacteria growth curve is quite low at increasing nanoparticle concentrations, and we started seeing growth inhibition after 15 to 30 min after inoculation. Gram-negative bacteria's log phase began to be influenced at 20 µg/mL nanoparticle concentration, but Gram-positive bacteria's log phase began at 60 µg/mL. As a result, Gram-positive bacteria's growth was mildly

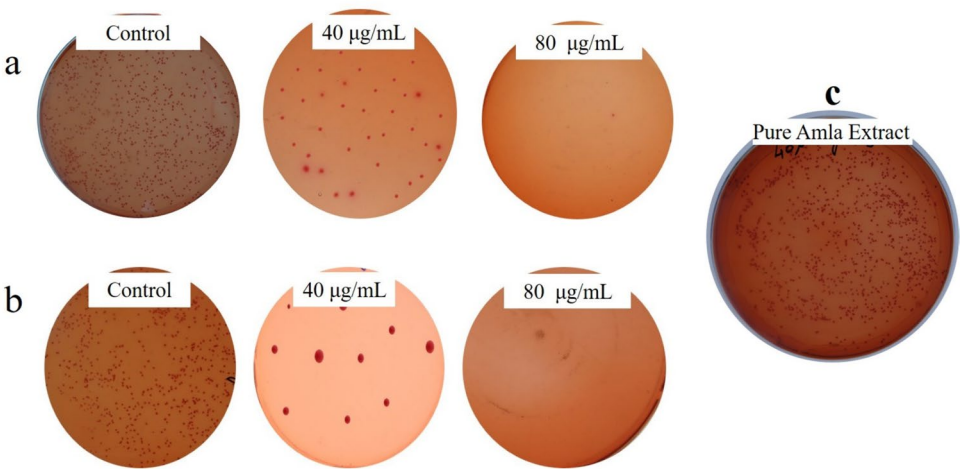

Fig. 7 Digital photographs of Ag NPs (0 to 80 µg/mL) on the growth of bacterial strains: **a** *E. coli*, **b** *S. aureus*, and **c** pure Amla extract on the growth of bacterial strain (*E. coli*)

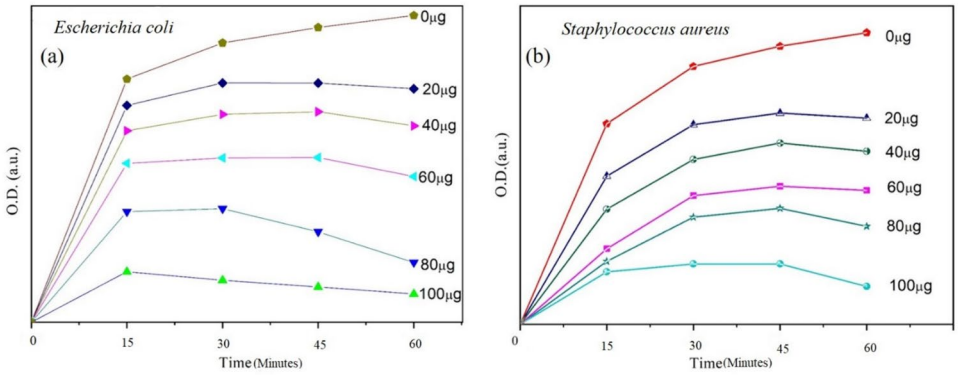

Fig. 8 Dynamic growth curves of different bacteria in LB media at different amounts of Ag NPs (0 to 100 μg/mL). **a** *E. coli* and **b** *S. aureus*

inhibited, whereas Gram-negative bacteria were more sensitive to the produced Ag NPs.

This significant antimicrobial activity of Ag NPs can be explained from some important physiological mechanisms related to Ag NPs. Since Ag NPs are positively charged particles, they can firmly attach to the negatively charged cell wall and membrane of bacteria [32]. Further, they may cause damage by penetrating the intracellular structures and bimolecular machinery of the cell [79]. After infiltration, they can cause further damage by interacting with the sulfur (S) and phosphorus (P) containing compounds (DNA/proteins) because of the high attraction of silver towards S and P. Moreover, it is found that both states of Ag, i.e., Ag^{+} and Ag^{0}, donate a significant contribution to the bactericidal activity, and it is anticipated that the Ag ions prevent protein synthesis and DNA replication. Furthermore, the reactive oxygen species (ROS) and free radicals generated from Ag NPs also caused toxicity in the bacterial culture [80]. A table for the comparative study of various nanoparticles and their biomedical application is given below (Table 1).

Conclusions

In conclusion, Ag NPs have been synthesized via a simple, environmentally friendly, and low-cost method using Amla extract as a reducing agent. TEM image analysis depicted polydispersity of Ag NPs with an average diameter in the range of 15–30 nm depending on the mixing ratio of $AgNO_3$ solution with Amla extract. The mechanism of silver reduction and NPs nucleation and growth has been explained in accordance with the literature data and experimental results. Antibacterial tests demonstrated that Amla-derived AgNPs prepared through a green process has significant antibacterial activity against both stains *E. coli* and *S. aureus*. This result encourages further studies on these green nanomaterials as potentially suitable candidates for development of antibacterial films for different purposes.

Table 1 Different types of metal oxide nanoparticles, plants used for their synthesis, and their biomedical applications

S. No	Metal oxide nanoparticles	Plant used for the synthesis	Biomedical applications	References
1	Gold (Au) NPs	Leaf, bark, stem, root, etc	Cancer theranostics	[81]
2	Copper oxide (CuO) NPs	*Giant milkweed*	Wound dressing	[82]
3	Iron (Fe) NPs	*Phoenix dactylifera*	Antibacterial activities	[83]
4	Copper (Cu) NPs	*Celastrus paniculatus* Willd. leaf extract	Photocatalytic and antifungal	[84]
5	Titanium dioxide (TiO_2) NPs	*Caricaceae* (papaya) shell extracts	Antifungal	[85]
6	Zinc (Zn) NPs	Sea-Lavender (Limonium pruinosum L. Chaz.) extract	Antiskin cancer, antimicrobial, and antioxidant	[86]
7	Magnesium (Mg) NPs	*Rosa floribunda charisma* extract	Antioxidant, antiaging, and antibiofilm	[87]
8	ZnO/CuO nanocomposites	*Calotropis gigantea* leaf extract	Wound dressing	[88]
9	ZnO/CuO nanocomposites	*Calotropis gigantea* leaf extract	Skin pathogens	[89]
10	Alginate (ALG) NPs	Honey	Drug delivery	[90]

Author Contribution A.N.Y. wrote the material synthesis section. P.S. wrote the biological part. S.U. and U.P.T. edited the manuscript. A.K.S. and A.S. conceptualized the experiments. P.S. worked on the mechanism.

Data Availability No datasets were generated or analyzed during the current study.

Declarations

Competing Interests The authors declare no competing interests.

References

1. Shao W, Liu X, Min H, Dong G, Feng Q, Zuo S (2015) Preparation, characterization, and antibacterial activity of silver nanoparticle-decorated graphene oxide nanocomposite. ACS Appl Mater Interfaces 7:6966–6973
2. Yadav AN, Jaiswal RK, Kumar P, Singh K (2020) Preparation, characterization, and antibacterial activity of ultrasmall chromium oxide nanocrystals. AIP Conf Proc 2265:030046
3. Daniel MC, Astruc D (2004) Gold nanoparticles: assembly, supramolecular chemistry, quantum-size-related properties, and applications toward biology, catalysis, and nanotechnology. Chem Rev 104:293–346
4. Barnes WL, Dereux A, Ebbesen TW (2003) Surface plasmon subwavelength optics. Nature 424:824–830
5. Gehr RJ, Boyd RW (1996) Optical properties of nanostructured optical materials. Chem Mater 8:1807–1819
6. Tripathi GNR (2003) p-Benzosemiquinone radical anion on silver nanoparticles in water. J Am Chem Soc 125:1178–1179
7. Lewis LN (1993) Chemical catalysis by colloids and clusters. Chem Rev 93:2693–2730
8. Singh AK, Tripathi YB, Pandey N, Singh DP, Tripathi D, Srivastava ON (2013) Enhanced antilipopolysaccharide (LPS) induced changes in macrophage functions by Rubia cordifolia (RC) embedded with Au nanoparticles. Free Radic Biol Med 65:217–223
9. Nomiya K, Yoshizawa A, Tsukagoshi K, Kasuga NC, Hirakawa S, Watanabe J (2004) Watanabe, Synthesis and structural characterization of silver(I), aluminium(III) and cobalt(II) complexes with 4-isopropyltropolone (hinokitiol) showing noteworthy biological activities. Action of silver (I)-oxygen bonding complexes on the antimicrobial activities. J. Inorg. Biochem 98:46–60
10. Gupta A, Silver S (1998) Silver as a biocide: will resistance become a problem? Nature Biotechnol 16:888–888
11. Roy K, Mao HQ, Huang SK, Leong KW (1999) Oral gene delivery with chitosan–DNA nanoparticles generates immunologic protection in a murine model of peanut allergy. Nat Med 5:387–391
12. Sachlos E, Gotora D, Czernuszka JT (2006) Collagen scaffolds reinforced with biomimetic composite nano-sized carbonate-substituted hydroxyapatite crystals and shaped by rapid prototyping to contain internal microchannels. Tissue Eng 12:2479–2487
13. Dakal TC, Kumar A, Majumdar RS, Yadav V (2016) Synthetic microbial ecology: engineering habitats for modular consortia. Front Microbiol 16:1831–1838
14. Beveridge TJ, Murray RG (1980) Sites of metal deposition in the cell wall of Bacillus subtilis. J Bacteriol 141:876–887
15. Slawson RM, Van Dyke MI, Lee H, Trevor JT (1992) Germanium and silver resistance, accumulation, and toxicity in microorganisms. Plasmid 27:73–79
16. Reese RN, Winge DR (1988) Sulfide stabilization of the cadmium-gamma-glutamyl peptide complex of Schizosaccharomyces pombe. J Biol Chem 263:12832–12835
17. Kowshik M, Vogel W, Urban J, Kulkarni SK, Paknikar KM (2002) Extracellular synthesis of silver nanoparticles by a silver-tolerant yeast strain MKY3. Adv Mater 14:815–818
18. Mukherjee P, Senapati S, Mandal D, Ahmad A, Khan MI, Kumar R, Sastry M (2002) Extracellular synthesis of gold nanoparticles by the fungus Fusarium oxysporum. ChemBioChem 3:461–463
19. Singh AK, Talat M, Singh DP, Srivastava ON (2010) Biosynthesis of gold and silver nanoparticles by natural precursor clove and their functionalization with amine group. J Nanopart Res 12:1667–1675
20. Dwivedi AD, Gopal K (2010) Biosynthesis of silver and gold nanoparticles using Chenopodium album leaf extract. Colloids Surf A 369:27–33
21. Huang JL, Li QB, Sun DH, Lu YH, Su YB, Yang X et al (2007) Biosynthesis of silver and gold nanoparticles by novel sundried Cinnamomum camphora leaf. Nanotechnology 18:105104
22. Saxena A, Tripathi R, Zafar F, Singh P (2011) Green synthesis of silver nanoparticles using aqueous solution of Ficus benghalensis leaf extract and characterization of their antibacterial activity. Mater Lett 67:91–94
23. Alahmad A, Feldhoff A, Bigall NC, Rusch P, Scheper T, Walter JG (2021) Hypericum perforatum L.-mediated green synthesis of silver nanoparticles exhibiting antioxidant and anticancer activities. Nanomaterials 11:487
24. Jain D, Daima HK, Kachhwaha S, Kothari S (2009) Synthesis of plant-mediated silver nanoparticles using papaya fruit extract and evaluation of their anti microbial activities. Dig J Nanomater Biostruct 4:557–563
25. Mallikarjuna K, Narasimha G, Dillip G, Praveen B, Shreedhar B, Lakshmi CS, Reddy B, Raju BDP (2011) Green synthesis of silver nanoparticles using Ocimum leaf extract and their characterization. Dig J Nanomater Biostruct 6:181–186
26. Li S, Shen Y, Xie A, Yu X, Qiu L, Zhang L, Zhang Q (2007) Green synthesis of silver nanoparticles using Capsicum annuum L. extract. Green Chem 9:852–858
27. Mallikarjuna K, Sushma NJ, Narasimha G, Manoj L, Raju BDP (2014) Phytochemical fabrication and characterization of silver nanoparticles by using Pepper leaf broth. Arab J Chem 7:1099–1103
28. Ahmed S, Ahmad M, Swami BL, Ikram S (2016) Green synthesis of silver nanoparticles using Azadirachta indica aqueous leaf extract. J Radiat Res Appl 9:1–7
29. Veerasamy R, Xin TZ, Gunasagaran S, Xiang TFW, Yang EFC, Jeyakumar N, Dhanaraj SA (2011) Biosynthesis of silver nanoparticles using mangosteen leaf extract and evaluation of their antimicrobial activities. J Saudi Chem Soc 15:113–120
30. Borah D, Kumar Yadav AA (2015) novel 'green'synthesis of antimicrobial silver nanoparticles (AgNPs) by using Garcinia morella(Gaertn) desr. fruit extract. Nanosci Nanotechnol Asia 5:25–31
31. Mehmood A, Murtaza G, Bhatti TM, Kausar R (2017) Phytomediated synthesis of silver nanoparticles from Melia azedarach L. leaf extract: characterization and antibacterial activity. Arab J Chem 10:S3048–S3053
32. Singh S, Vidyasagar G (2014) Green synthesis, characterization and antimicrobial activity of silver nanoparticles by using Sterculia foetida L. young leaves aqueous extract. Int J Green Chem Bioprocess 4:5
33. Vijistella Bai G (2014) Green synthesis of silver nanostructures against human cancer cell lines and certain pathogens. Int J Pharm Chem Biol Sci 4:101–111

34. Kalidasan M, Yogamoorthi A (2014) Biosynthesis of silver nanoparticles using Achyranthus aspera and its characterization. Int J Nanomater Biostruct 4:5–11
35. Jayapriya E, Lalitha P (2013) Synthesis of silver nanoparticles using leaf aqueous extract of Ocimum basilicum (L.). Int J Chemtech Res 5:2985–2992
36. Ahmad N, Sharma S, Rai R (2012) Rapid green synthesis of silver and gold nanoparticles using peels of Punica granatum. Adv Mater Lett 3:376–380
37. Ponarulselvam S, Panneerselvam C, Murugan K, Aarthi N, Kalimuthu K, Thangamani S (2012) Synthesis of silver nanoparticles using leaves of Catharanthus roseus Linn. G. Don and their antiplasmodial activities. Asian Pac J Trop Biomed 2:574–580
38. Jyoti K, Baunthiyal M (2019) Singh, A. Characterization of silver nanoparticles synthesized using Urtica dioica Linn. leaves and their synergistic effects with antibiotics. J Radiat Res Appl Sci 9:217–227
39. Mohapatra B, Kuriakose S, Mohapatra S (2015) Rapid green synthesis of silver nanoparticles and nanorods using Piper nigrum extract. J Alloys Compd 637:119–126
40. Chung IM, Park I, Seung-Hyun K, Thiruvengadam M, Rajakumar G (2016) Plant- mediated synthesis of silver nanoparticles: their characteristic properties and therapeutic applications. Nanoscale Res Lett 11:40
41. Mishra M, Chauhan P (2015) Nanosilver and its medical implications. J Nanomed Res 2:1–10
42. Demchenko AG, Sadykova VS, Lyundup AV, Sedyakina NE, Gromovykh TI, Feldman NB, Ananyan MA, Lutsenko SV (2020) Antimicrobial and cytotoxic activity of silver nanoparticles stabilized by natural biopolymer arabinogalactan. Int J Nanosci 19(04):1950029
43. Rosarin FS, Arulmozhi V, Nagarajan S, Mirunalini S (2013) Antiproliferative effect of silver nanoparticles synthesized using amla on Hep2 cell line. Asian Pac J Trop Med 6(1):1–10. https://doi.org/10.1016/S1995-7645(12)60193-X
44. Iqbal N, Iqubal SS, Khan AA, Mohammed T, Alshabi AM, Aazam ES, Rafiquee MZA (2021) Effect of CTABr (surfactant) on the kinetics of formation of silver nanoparticles by Amla extract. J Mol Liq 329:115537
45. Ramesh PS, Kokila T, Geetha D (2015) Plant mediated green synthesis and antibacterial activity of silver nanoparticles using Emblica officinalis fruit extract. Spectrochim Acta Part A Mol Biomol Spectrosc 142:339–343
46. Singh AK, Tripathi M, Srivastava ON, Verma RK (2017) Silver nanoparticles/gelatin composite: a new class of antibacterial material. Chemistry Select 2:7233–7238
47. Singh AK, Srivastava ON (2015) One-step green synthesis of gold nanoparticles using black cardamom and effect of pH on its synthesis. Nanoscale Res Lett 10:1–12
48. Yadav AN, Singh AK, Chauhan D, Solanki PR, Kumar P, Singh K (2020) Evaluation of dopant energy and Stokes shift in Cu-doped CdS quantum dots via spectro-electrochemical probing. New J Chem 44:13529–13533
49. Yadav AN, Singh AK, Srivastava S, Kumar M, Gupta BK, Singh K (2019) Ultrafast charge carrier dynamics in CdSe/V_2O_5 core/shell quantum dots. Phys Chem Chem Phys 21:6265–6273
50. Jyoti K, Baunthiyal M, Singh A (2016) Characterization of silver nanoparticles synthesized using Urtica dioica Linn. leaves and their synergistic effects with antibiotics. J Radiat Res Appl Sci 9:217–227
51. Mie G (1908) Contributions to the optics of turbid media, especially colloidal metal solutions. Ann Phys 25:377–445
52. Huang J, Li Q, Sun D, Yinghua Lu, Yuanbo Su, Yang X, Wang H, Wang Y, Shao W, He N (2007) Jinqing Hong and Cuixue Nanotechnology 18:1–11
53. Alahmad A, Feldhoff, A, Bigall NC, Rusch P, Scheper T, Walter JG (2021) Hypericum perforatum L.-mediated green synthesis of silver nanoparticles exhibiting antioxidant and anticancer activities. Nanomaterials 11:487
54. Scroccarello A, Molina-Hernández B, Della Pelle F, Ciancetta J, Ferraro G, Fratini E, Valbonetti L, Chaves C, Copez, D (2021) Compagnone, Effect of phenolic compounds-capped AgNPs on growth inhibition of Aspergillus niger, Colloids and Surfaces B: Biointerfaces 199:111533
55. El-Seedi HR, El-Shabasyde RM, Khalifafg SAM, Saeedh A, Shah A, Shahj R, Iftikharh FJ, Abdel-Daim MM, Omrilm A, Hajrahandlm NH, Sabirlm JSM, Zou X, Halabic MF, Sarhann M, Guo W (2019) Metal nanoparticles fabricated by green chemistry using natural extracts: biosynthesis, mechanisms, and applications. RSC Adv 9:24539–24559
56. Thakkar KN, Mhatre SS, Parikh RY (2010) Biological synthesis of metallic nanoparticles, Nanomedicine: Nanotechnology. Biology and Medicine 6(2):257–262
57. Thakkar KN, Mhatre SS, Parikh RY (2010) Biological synthesis of metallic nanoparticles. Nanomedicine 6:257–262
58. Duran N, Marcato PD, Duran M, Yadav A, Gada A, Rai M (2011) Mechanistic aspects in the biogenic synthesis of extracellular metal nanoparticles by peptides, bacteria, fungi, and plants. Appl Microbiol Biotechnol 90:1609–1624
59. Variya BC, Bakrania AK, Patel SS (2016) Emblica officinalis (Amla): A review for its phytochemistry, ethnomedicinal uses and medicinal potentials with respect to molecular mechanisms. Pharmacol Res 111:180–200
60. Gantait S, Mahanta M, Bera, S. et al (2021) Advances in biotechnology of Emblica officinalis Gaertn. syn. Phyllanthus emblica L.: a nutraceuticals-rich fruit tree with multifaceted ethnomedicinal uses. 3 Biotech 11:62
61. Olennikov DN, Kashchenko NI, Schwabl H et al (2015) New mucic acid gallates from Phyllanthus emblica. Chem Nat Compd 51:666–670
62. Li Y, Guo B, Wang W, Li L, Cao L, Yang C, Liu J, Liang Q, Chen J (2019) Shaohua Wu & Liaoyuan Zhang Characterization of phenolic compounds from Phyllanthusemblica fruits using HPLC-ESI-TOF-MS as affected by an optimized microwave-assisted extraction. Int J Food Prop 22(1):330–342
63. Ferraris M, Miola A, Cochis B, Azzimonti L, Rimondini E, Prenesti E (2017) Vernè, In situ reduction of antibacterial silver ions to metallic silver nanoparticles on bioactive glasses functionalized with polyphenols. Appl Surf Sci 396:461–470
64. Chokkareddy R, Redhi GG (2018) Green synthesis of metal nanoparticles and its reaction mechanisms. In Green Metal Nanoparticles: Synthesis, Characterization and Their Application, Kanchi S, Ahmed S Eds. Scrivener Publishing LLC: Beverly, MA, USA 113–139. ISBN 978–1–119–41887–0
65. Makarov VV et al (2014) "Green" nanotechnologies: synthesis of metal nanoparticles using plants. Acta Naturae 6:35–44
66. Jain S, Mehata MS (2017) Medicinal plant leaf extract and pure flavonoid mediated green synthesis of silver nanoparticles and their enhanced antibacterial property. Sci Rep 7:15867
67. Hatanaka M (2013) Through-bond instability in polyphenol tautomers. Tetrahedron Lett 54:1452–1455
68. Rao KJ, Paria S (2013) Green synthesis of silver nanoparticles from aqueous Aegle marmelos leaf extract. Mater Res Bull 48:628–634
69. Harada M, Katagiri E (2010) Mechanism of silver particle formation during photoreduction using in situ time-resolved SAXS analysis. Langmuir 26(23):17896–17905. https://doi.org/10.1021/la102705h
70. Rodríguez-Sánchez ML, Rodríguez MJ, Blanco MC, Rivas J, López-Quintela MA (2005) Kinetics and mechanism of the formation of Ag nanoparticles by electrochemical techniques: a plasmon and cluster time-resolved spectroscopic study. J Phys Chem B 109:1183–1191

71. Dakal TC, Kumar A, Majumdar RS, Yadav V (1831) Mechanistic basis of antimicrobial actions of silver nanoparticles. Front Microbiol 2016:7
72. El-Seedi HR, El-Shabasyde RM, Khalifafg SAM, Saeedh A, Shah A, Shahj R, Iftikharh FJ, Abdel-Daim MM, Omrilm A, Hajrahandlm NH, Sabirlm JSM, Zou X, Halabic MF, Sarhann W, Guo W (2019) Metal nanoparticles fabricated by green chemistry using natural extracts: biosynthesis, mechanisms, and applications. RSC Adv 9:24539
73. Das S, Langbang L, Haque M (2020) Vinay Kumar Belwal, Kripamoy Aguan, Atanu Singha Roy, Biocompatible silver nanoparticles: an investigation into their protein binding efficacies, anti-bacterial effects and cell cytotoxicity studies. J Pharm Anal. https://doi.org/10.1016/j.jpha.2020.12.003
74. characterization and stability study (2017) Patel, K Role of stabilizing agents in the formation of stable silver nanoparticles in aqueous solution. J Dispersion Sci Technol 38:626–631
75. Luo W, Zhao M, Yang B, Ren J, Shen G, Rao G (2011) Antioxidant and antiproliferative capacities of phenolics purified from Phyllanthus emblica L. fruit. Food Chem 126:277–282. https://doi.org/10.1016/j.foodchem.2010.11.018
76. Raghavan BS, Kondath S, Anantanarayanan R et al (2015) Kaempferol mediated synthesis of gold nanoparticles and their cytotoxic effects on MCF-7 cancer cell line Process. Biochem 50:1966–1976
77. Guo L, Nie J, Du B, Peng Z, Tesche B, Kleinermanns K (2008) Thermoresponsive polymer- stabilized silver nanoparticles. J Colloid Interface Sci 319:175–181
78. Rai M, Yadav A, Gade A (2009) Silver nanoparticles as a new generation of antimicrobials. Biotech Advanc 27:76–83
79. Pal S, Tak Y, Song J (2007) Does the antibacterial activity of silver nanoparticles depend on the shape of the nanoparticles? A study of the gram-negative bacterium Escherichia coli. Appl Environ Microbiol 73:1712–1720
80. Guzman M, Dille J, Godet S (2012) Synthesis and antibacterial activity of silver nanoparticles against gram-positive and gram-negative bacteria. Nanomedicine 8:37–45
81. Bharadwaj KK, Rabha B, Pati S, Sarkar T, Choudhury BK, Barman A, Bhattacharjya D, Srivastava A, Baishya D, Edinur HA, Kari ZA, Noor NHM (2021) Green synthesis of gold nanoparticles using plant extracts as beneficial prospect for cancer theranostics. Molecules 26:6389
82. Govindasamy GA, Mydin RBSMN, Harun NH, Effendy WNFWE, Sreekantan S (2023) Giant milkweed plant-based copper oxide nanoparticles for wound dressing application: physicochemical, bactericidal and cytocompatibility profiles. Chem Pap 77:1181
83. Batool F, Iqbal MS, Khan S-U-D, Khan J, Ahmed B, Qadir MI (2021) Biologically synthesized iron nanoparticles (FeNPs) from Phoenix dactylifera have anti-bacterial activities. Sci Rep 11:22132
84. Mali SC, Dhaka A, Githala CK, Trivedi R, (2020) Green synthesis of copper nanoparticles using Celastrus paniculatus Willd. leaf extract and their photocatalytic and antifungal properties. Biotechnol Reports 27:e00518
85. Saka A, Shifera Y, Jule LT, Badassa B, Nagaprasad N, Shanmugam R, Dwarampudi LP, Seenivasan V, Ramaswamy K (2022) Biosynthesis of TiO2 nanoparticles by Caricaceae (Papaya) shell extracts for antifungal application. Sci Rep 12:15960
86. Naiel B, Fawzy M, Halmy MWA, Mahmoud AED (2022) Green synthesis of zinc oxide nanoparticles using sea lavender (Limonium pruinosum L. Chaz.) extract: characterization, evaluation of anti-skin cancer, antimicrobial and antioxidant potentials. Sci Rep 12:20370
87. Younis IY, El-Hawary SS, Eldahshan OA, Abdel-Aziz MM, Ali ZY (2021) Green synthesis of magnesium nanoparticles mediated from Rosa floribunda charisma extract and its antioxidant, antiaging and antibiofilm activities. Sci Rep 11:16868
88. Govindasamy GA, Mydin RBSMN, Effendy WNFWE, Sreekantan S (2022) Novel dual-ionic ZnO/CuO embedded in porous chitosan biopolymer for wound dressing application: physicochemical, bactericidal, cytocompatibility and wound healing profiles. Mater Today Commun 33:104545
89. Govindasamy GA, Mydin RBSMN, Sreekantan S, Harun NH (2021) Compositions and antimicrobial properties of binary ZnO–CuO nanocomposites encapsulated calcium and carbon from Calotropis gigantea targeted for skin pathogens. Sci Rep 11:99
90. Thomas D, Thomas KK, Latha MS (2020) Preparation and evaluation of alginate nanoparticles prepared by green method for drug delivery applications. Int J Biol Macromol 154:888